HER3 PET Imaging Identifies HER2+ Breast Cancers That Benefit From HER3 Inhibitor Addition

Eric Wehrenberg-Klee
Massachusetts General Hospital https://orcid.org/0000-0002-4712-3986
Nicoleta Sinevici
Massachusetts General Hospital
Sarah Nesti
Massachusetts General Hospital
Taylor Kalomeris
Massachusetts General Hospital
Emily Austin
Massachusetts General Hospital
Benjamin Larimer
Massachusetts General Hospital
Umar Mahmood (umahmodd@mgh.harvard.edu)
Center for Biomedical Imaging, Department of Radiology, Massachusetts General Hospital, Boston, Massachusetts

Research article

Keywords: HER3, HER2, lapatinib, imaging, PET, breast cancer, precision medicine

Posted Date: December 12th, 2020

DOI: https://doi.org/10.21203/rs.3.rs-125139/v1

Abstract

Background: Standard therapy for HER2+ breast cancers includes HER2 inhibition. While HER2 inhibitors have modestly improved outcomes, they have not had nearly the original anticipated therapeutic efficacy, with only a modest improvement in survival in both the metastatic and adjuvant setting. An important intrinsic resistance mechanism to HER2 inhibition in some breast cancers is dynamic upregulation of HER3. Increase in HER3 expression that occurs in response to HER2 inhibition allows for continued growth signaling through HER2:HER3 heterodimers, promoting tumor escape. We hypothesized that a non-invasive method to image changes in HER3 expression would be valuable to identify those breast cancers that dynamically upregulate HER3 in response to HER2 inhibition. We further hypothesized that this imaging method could identify those tumors that would benefit by further addition of a HER3 inhibitor.

Methods: In cells treated with the HER2 inhibitor lapatinib, we evaluate changes in HER3 expression and viability. Mouse HER2+ breast cancer models treated with lapatinib were imaged with a peptide-based HER3-specific PET imaging agent (Ga-68-HER3P1) to assess for dynamic changes in tumoral HER3 expression and uptake confirmed by biodistribution. Subsequently, HER2+ cell lines were treated with the HER2 inhibitor lapatinib as well HER3-specific siRNA to assess for changes in viability and correlate with HER3 expression upregulation. For all statistical comparisons, $p<0.05$ was considered statistically significant.

Results: Ga68-HER3P1 PET imaging of mice implanted with the HER2+ breast cancer cell lines MDA-MB453 or HCC-1569 prior to and after treatment with lapatinib demonstrated a significant increase in SUV in MDA-MB453 tumors only, consistent with in vitro findings. The addition of HER3 siRNA to lapatinib increased therapeutic efficacy in MDA-MB453 cells, but not in HCC-1569 cells.

Conclusion: HER3 PET imaging can be used to visualize dynamic changes in HER3 expression that occur in HER2+ breast cancers with HER2 inhibitor treatment and identify those likely to benefit by the addition of combination HER3 and HER2 inhibition.

Introduction

In HER2 + breast cancer, overexpression and overactivity of the surface-expressed receptor tyrosine kinase human-epidermal growth factor receptor 2 (HER2) is an important driver of cancer growth. Multiple therapeutic inhibitors of HER2 have been brought into clinical practice, including the therapeutic antibodies trastuzumab and pertuzumab, the antibody-drug-conjugate trastuzumab emtansine, and the small molecule tyrosine kinase inhibitors lapatinib and neratinib(1–5). These therapies are the standard of care for HER2 + breast cancer and have been used to treat more than 2 million patients. Although these therapies have represented an improvement over standard chemotherapy, their efficacy has been lower than originally hypothesized. Response rates range from 4–51% depending on line of therapy, and as a result only modestly improve overall survival (6, 7). The less than anticipated efficacy has been shown to

be due to multiple resistance mechanisms, including mutations in HER2 and downstream pathways, some of which are acquired with prolonged treatment(8–14). In contrast to these mechanisms of acquired resistance, a very important mechanism of intrinsic resistance that also limits efficacy involves the closely related receptor tyrosine kinase HER3. HER3 forms active heterodimers with HER2 (HER2:HER3) that can transmit growth signals along the PI3K◊AKT◊MAPK signaling pathway(15). At baseline, tumoral expression of HER3 is typically low, and signaling is predominantly through HER2:HER2 homodimers(16). However, with therapeutic inhibition of HER2 there can be rapid compensatory increase in HER3 surface expression, resulting in HER2:HER3 heterodimer formation, with increased expression observed within 24 hours of exposure (17). In tumors that can dynamically upregulate HER3, this pathway restores growth pathway signaling and mediates resistance to HER2 inhibition(16–20). Previous preclinical studies have demonstrated a wide range of HER3 expression change across cell lines with HER2 inhibition, suggesting that this resistance mechanism may only be active in a fraction of HER2 + tumors. These same studies have also shown that dynamic increase in HER3 expression can be seen in both lapatinib 'sensitive' and 'resistant' cell lines, implying opportunity for therapeutic improvement in both categories. Of importance, these mechanisms have been elucidated using the orally available HER2 tyrosine kinase inhibitor lapatinib that binds to the intracellular kinase domain rather than HER2-specific antibodies which are thought to have multiple modes of therapeutic action (21).

For HER2 + patients being treated with a HER2 inhibitor, HER3-specific positron-emission tomography (PET) imaging that provided a readout of total tumoral HER3 expression across the body could be used to non-invasively evaluate the activity of this resistance pathway. A pre-treatment HER3 PET scan could establish baseline HER3 expression across all sites of disease. A repeat on-treatment HER3 PET scan obtained after a dose or several doses of HER2 inhibitor could then assess for the degree of HER3 expression increase over baseline. The degree of HER3 increase may be indicative of the degree to which HER3 is mediating resistance to HER2 inhibition in any given patient. Furthermore, by identifying those patients in which HER3 contributes to HER2 inhibitor resistance, a HER3 PET imaging agent may identify those patients most likely to benefit from the therapeutic addition of a HER3 inhibitor. Several HER3 inhibitors have been investigated clinically, but the only HER3 inhibitor under active clinical investigation to our knowledge is the antibody drug conjugate U3-1402 (22).

We have previously developed a HER3-specific PET imaging agent (HER3P1) that allows for non-invasive in vivo assessment of tumoral HER3 expression(23). This agent is derived from a 7 amino-acid peptide identified through phage-display found to bind to HER3 with 270 nM affinity. Peptide-based agents have rapid pharmacokinetics with renal excretion that make them ideal for repeat imaging, as the imaging agent is entirely cleared within hours of injection.

In this study we present preclinical data to support the potential role of HER3 PET imaging in guiding therapy for metastatic HER2 + breast cancer. In a panel of HER2-overexpressing cell lines treated with the HER2 inhibitor lapatinib we show that HER3 expression increases post-treatment in some but not all cell lines. We also demonstrate that increase in HER3 expression is seen in cell lines classified as both 'sensitive' and 'resistant' to HER3 inhibition; suggesting that the addition of a HER3 inhibitor could further

improve efficacy in these tumors. From this panel we select resistant cell lines that either upregulated HER3 or showed minimal change in HER3 expression in vitro, and demonstrate that our HER3 PET imaging agent can be used to image these scenarios in vivo. We extend our findings by demonstrating that the addition of HER3-knockdown siRNA to HER2 inhibition significantly increases cell-killing in a cell-line that upregulates HER3, but not in a cell line that had showed no change in HER3 expression. These data suggest that HER3 PET imaging could be used to non-invasively identify HER2 + breast cancers that resist HER2 inhibition through dynamic upregulation of HER3, and simultaneously select those patients who could benefit by the addition of a HER3 inhibitor to therapy in the future.

Methods

Cell Culture

The HER2 + human breast carcinoma cell lines SKBR-3, BT-474, HCC1954, HCC1569, MDA-MB-453 were obtained from the American Type Culture Collection. The HER2 + human breast carcinoma cell line JIMT-1 was obtained from Leibniz Institute DSMZ-German Collection of Microorganisms and Cell Cultures. All cell lines except HCC1954 were HER3+. All cell lines were tested for Mycoplasma contamination using PCR (LookOut Mycoplasma PCR Detection Kit; Sigma). Cell lines were cultured in Leibovitz L-15 medium, RPMI-1640 medium, or Eagle minimum essential medium as appropriate and supplemented by 20% (v/v) fetal bovine serum, penicillin (100 U/mL), and streptomycin (100 mg/mL). Cells were maintained in a humidified atmosphere of 5% CO2 at 37C. Subculturing was performed using a 0.25% trypsin-0.1% ethylenediaminetetraacetic acid solution.

Western Blots

Primary antibodies were to HER3/ErbB3, pHER3, HER2, pHER2, PI3K, pPI3K, AKT, pAKT, MAPK, pMAPK, and ß-actin rabbit mAb antibody (all obtained from either Santa Cruz Biotech or Cell Signaling Technology). For semi-quantitative analysis, bands were quantified and normalized to ß -actin bands with Carestream spectral imaging software (Carestream) and analyzed on ImageJ software (NIH). Cells were treated with either vehicle or 200 nM lapatinib (purchased from LC laboratories) for 48 h. Medium with fresh lapatinib was changed every 24 hours. All cell studies were repeated in triplicate.

Cell-Viability Assay

Cell growth was assayed by seeding 5,000 cells per well in a 96- well culture plate. After 24 hours, cells were treated with 200 nM lapatinib or vehicle only. 200 nM lapatinib chosen as has been previously defined as the threshold to determine lapatinib resistance among HER2 + cancer cells (24). Medium with fresh lapatinib was changed every 24 hours. Note that for all of our studies, lapatinib was selected as the treatment of choice over HER2 inhibiting antibodies due to concern that antibodies may have multiple modes of therapeutic efficacy that could potentially confound result interpretation. Daily cell viability from triplicate wells was assessed using Cell-Titer Glo assay (Promega) according to manufacturer

protocol over 5 days of treatment, with luminescence assessed on a Promega GloMax Discover Microplate Reader. Cell viability is reported as a percentage relative to vehicle-treated cells.

Ga68-HER3P1 Preparation

The NOTA-conjugated peptide HER3P1 (NOTA-ßAGGG-CLPTKFRSC) with 270 nM affinity for HER3 was synthesized as described previously(23). The peptide was radiolabeled with the radiometal ^{68}Ga eluted from a ^{68}Ge/^{68}Ga generator (RadioMedix, Houston, TX) with 0.1M HCl. The eluent was raised to pH 3.5-4.0 with 2M HEPES before addition of 100 µg of NOTA-HER3P1. After allowing the labeling reaction to proceed for 10 minutes at room temperature, the peptide was purified on a reverse phase C18 Sep-Pak mini cartridge (Waters, Milford, MA) and eluted in 200 µL 70% ethanol. Radiochemical purity was determined by ITLC. Saline was added to create a final formulation of < 10% ethanol concentration and approximately 9.5–28 MBq with 50 µg peptide injected per mouse.

Mouse Studies:

Female SCID mice bearing either MDA-MB-453 or HCC-1569 tumors were implanted in the right upper flank of mice and grown to approximately 100mm^3. The HER2 + cell lines selected for further study are both resistant to HER2 inhibition, yet only MDA-MB-453 demonstrated significant increase in HER3 expression in our western blots. Mice with each tumor type were randomized into two treatment groups: saline vehicle, or lapatinib treatment. 100 mg/kg lapatinib was administered as a suspension in 0.5% hydroxypropylmethylcellulose and 0.2% Tween 80 by oral gavage in two divided daily doses for two days. This dosing has previously been determined as the maximum tolerated dose of lapatinib for continuous dosing (16). Treatment duration was based upon results of HER3 upregulation observed in in vitro studies.

HER3P1 Biodistribution

Groups of four mice with either MDA-MB-453 or HCC-1569 randomized to vehicle or lapatinib treatment as described above were analyzed. NOTA-HER3P1 was radiolabeled with Ga-68 and purified to > 95% purity by reverse phase chromatography, as determined by ITLC and then 50 µg injected intravenously via tail vein injection and allowed to circulate for 1 h prior to euthanization. Circulation time chosen to account for the short circulation time of peptides and short half-life of Ga-68. Tumors and relevant organs were removed from mice, weighed, and total activity for each was quantified by a Wallac gamma counter (Perkin Elmer, Waltham, MA) using the decay-corrected injected dose and expressed percentage of injected dose per gram (%ID/g). After radioactive decay, tumors were lysed and analyzed by Western blot for correlation of tumor uptake to HER3 expression normalized to β-actin. HER3 (sc-81455, Santa Cruz Biotech, Dallas, TX) and β-actin (13E5, Cell Signaling, Danvers, MA) antibodies were used to detect protein followed by an HRP-conjugated goat-antirabbit secondary antibody (Abcam) and detection by SignalFire chemiluminescent substrate (Cell Signaling).

HER3P1 PET Imaging:

Female SCID mice bearing MDA-MB-453 tumors (6 mice) were implanted in the right upper flank of mice and grown to approximately 100mm^3. Imaging agent was prepared as above, and mice were subsequently injected with 50 µg Ga-68 HER3P1 via tail vein. Imaging agent was allowed to circulate for one hour. Mice were then imaged on a rodent Triumph PET/CT (GE Healthcare, Wilmington, MA). PET images were acquired for 15 min and followed by CT acquisition. Reconstruction was achieved using 3D-MLEM (4 iterations, 20 subsets) and corrected for scatter and randoms. Subsequently, all mice were treated with 100 mg/kg lapatinib daily, prepared as above, by oral gavage administered twice daily for two days. Mice were then reinjected with 50 µg Ga-68 HER3P1 and again underwent PET/CT imaging. The tumor and blood uptake were calculated in a 3D region of interest drawn around the tumor and heart, respectively, using CT guidance. VivoQuant software (InviCRO, Boston, MA) was used for image processing and analysis. Individual tumors were identified manually by drawing a 3D region of interest using CT-anatomic correlation. Background blood pool radioactivity was measured by identifying the left ventricle of the heart as a region of interest.

HER3 siRNA Knockdown:

HER3 knockdown was achieved using the oligonucleotide sequences of small interfering siRNA targeted to murine Erbb3 (M-040415-01, SMARTpool siGENOME siRNA, Dharmacon) as per manufacturer guidelines. In short, MDA-MB 453 and HCC-1569 cells were seeded overnight prior to transfection. Cells were seeded at a density of 1.5×10^4 (96 well plate) or 5×10^5 cells (6 well plate) in complete media. Cells were transfected with 0.2 µl of DharmaFect (Dharmacon) and 10–30 nM of HER3 siRNA or non-targeting siRNA (siRNA nontargeting pool #2, Dharmacon) as indicated. Degree of HER3 mRNA knockdown was determined by HER3 mRNA PCR. 24 h post transfection, cells were treated with 200 nM lapatinib in fresh medium. Lapatinib treatments continued every 24 h for a total of 120 h. Daily cell counts from triplicate wells were obtained for 5 days with a hematocytometer. Cell growth is reported as a percentage relative to control cell count on the same day.

Results

Treatment of an array of HER2 + breast cancer cell lines with 200 nM lapatinib demonstrated an increase in HER3 expression compared with vehicle-treated cells in some but not all HER2 + cell lines (Fig. 1A), confirming that HER3 upregulation in the presence of HER2 inhibition is not a universal feature of HER2 + breast cancer cell-lines. Indeed, interpreted in conjunction with cell-viability data of the same cell lines treated for 5 days with 200 nM lapatinib (Fig. 1B), increased HER3 expression is seen among both classically ‘sensitive’ HER2 lines such as SK-BR3 and BT-474 as well as the ‘resistant’ line MDA-MB-453(25), consistent with definitions of lapatinib sensitivity described by Wetterskog et al(24) and Konecny et al(26). Other resistant HER2 + lines that did not show meaningful increase in HER3 expression include JIMT-1 (resistance mechanisms known to include activating PIK3CA gene, low PTEN expression, high NRG1 expression and relatively low expression of HER2 despite gene amplification) (27); HCC-1569 (complete PTEN loss) (28); and HCC-1954, which has been previously shown by us and others to have no/low HER3 expression (23, 29)

We sought to demonstrate that our previously developed HER3 PET imaging agent (23) could quantify the changes in HER3 expression that occur in vivo with lapatinib treatment. Mice were implanted with either the cell line MDA-MB-453 or HCC-1569. As discussed, in our *in vitro* studies lapatinib treatment induced an increase in HER3 expression in MDA-MB-453 cells, but not in HCC-1569 relative to vehicle treated tumors. Bio-distribution studies showed that Ga68-HER3P1 could quantify the dynamic increase in HER3 expression that occurs with lapatinib treatment (Fig. 2). Comparison of vehicle-treated and lapatinib-treated bio-distributions demonstrated a low baseline uptake of HER3P1 tracer in both MDA-MB-453 tumors (0.09%ID/g, SD = 0.02%) and HCC-1569 tumors (0.05%ID/g, SD = 0.01%). In MDA-MB-453 tumors, lapatinib treatment resulted in a significant increase in tracer uptake to 0.29%ID/g (SD = 0.04%, P = 0.04 by unpaired T-test), whereas the change in HCC-1569 tumors to 0.09% ID/g (SD = 0.05%, P = 0.24 by unpaired T-test) was non-significant (Fig. 2C). No other significant alterations in organ biodistribution were seen between vehicle and treatment groups, and distribution is within expected distribution for a peptide based radio-tracer with high percentage of renal uptake representing renal excretion. Findings of biodistribution studies are comparable to HER3 Western blot analysis of excised tumors, which shows a significant increase in normalized HER3 in MDA-MB-453 tumors with lapatinib treatment that demonstrated a normalized HER3 of 1.2 (+/-0.6) for vehicle vs 3.1 (+/- 0.8) for treated tumors (P = 0.04 by unpaired T-test), but not in HCC-1569 tumors, with normalized HER3 of 1.7 (+/-0.8) for vehicle vs 2.0 (+/-0.4) for treated tumors (P = 0.45 by unpaired T-test) (Fig. 2D).

We then sought to show that changes in tumoral HER3 uptake could be imaged on an individual tumor basis. Mice injected with MDA-MB-453 were injected with Ga68-HER3P1 and imaged one hour later. Mice were then treated with twice-daily lapatinib oral gavage for two days. Mice were then reinjected with Ga68-HER3P1 and imaged one-hour later. A representative image of a MDA-MB-453 mouse imaged on day 0 and scanned again 48 hours later demonstrates increased Ga68-HER3P1 uptake within the tumor post-treatment (Fig. 3A, B). Comparison of pre-treatment and post-treatment SUVmax demonstrates an increase in uptake of Ga-68-HER3P1 in all imaged tumors. Group mean SUVmax increased from 0.07 (SD = 0.03) pre treatment to 0.22 (SD = 0.06) post-treatment (P = 0.02 by Wilcoxon matched-pairs signed rank test), a nearly three-fold increase (Fig. 3C).

We then extended our imaging findings to suggest the possible future role of HER3 PET imaging to dynamically guide therapeutic decisions for breast cancer. Both HER2 + cell lines we had selected for imaging, MDA-MB-453 and HCC-1569, are resistant to HER2 inhibition, yet only MDA-MB-453 demonstrates significant increase in HER3 expression. This difference in HER3 expression upregulation in response to HER2 inhibition suggests different mechanisms of HER2 resistance, and indeed HCC-1569 resistance to HER2 inhibition is rather mediated by PTEN loss(28). We hypothesized that tumor cell lines that upregulate HER3 expression in response to HER2 inhibition would be sensitive to additional HER3 inhibition, whereas tumor cell lines that do not increase HER3 expression under similar treatment conditions would not. To test this hypothesis, we treated both MDA-MB-453 cells and HCC1569 cells with lapatinib in addition to HER3-targeting siRNA. HER3 targeting siRNA reduced HER3 mRNA by 66% (1% SD) in MDAMB453 (P = 0.01 by unpaired T-Test) and by 66% (1% SD) in HCC1569 cells relative to non-targeting siRNA (P = 0.01 by unpaired T-Test) (Fig. 4A, B). For HCC-1569 cells the addition of HER3 siRNA

to lapatinib therapy had no significant effect on cell growth, with growth of 73% (SD = 30%) for dual treated relative to 88% (SD = 18%) for lapatinib treated and 78% (SD = 21%) for HER3 siRNA treated tumors (P = 0.6 determined by 2-way ANOVA) (Fig. 4C). By contrast, for MDA-MB-453 cells, five days of treatment with both lapatinib and HER3 siRNA significantly impaired growth relative to both lapatinib monotherapy and HER3 siRNA monotherapy. Dual-treated (lapatinib + HER3 siRNA) cells had 37% (SD = 19%) growth relative to vehicle-treated cells, whereas treatment with lapatinib alone (93% relative growth, SD = 35%) or HER3 siRNA alone (94% relative growth, SD 36%) was similar to vehicle-treated cells ($P < 0.001$ as determined by 2-way ANOVA) (Fig. 4D).

Discussion

The survival and growth of HER2 + breast cancer is highly reliant upon signaling through the HER2/PI3K/AKT pathway. Significant preclinical evidence points to the role of the related receptor HER3 in mediating resistance to HER2 inhibitors. Shortly following the initial inhibition of HER2 there is dynamic upregulation of HER3 expression through a variety of pre and post-translational mechanisms. The increased HER3 expression allows HER2:HER3 heterodimer formation that in turn allows for persistent signaling through the HER2/PI3K/AKT pathway. This resistance mechanism is so robust that in one in vitro study, 100x the clinical concentration of the HER2 inhibitor lapatinib is required to completely eradicate HER2 pathway signaling (16), and dual treatment with trastuzumab and lapatinib was unable to completely eradicate HER3 signaling in another(30).

In this preclinical study, we sought to demonstrate that HER3 PET imaging with Ga-68 HER3P1 could image the changes in HER3 expression that occur rapidly during treatment with the HER2 inhibitor lapatinib. These data show that HER3 PET imaging can serve as a non-invasive method of assessing dynamic changes in HER3 expression, and thereby has the ability guide therapeutic regimen choice. We had previously reported on antibody-based HER3 PET imaging, showing that the upregulation of HER3 in triple negative breast cancers in response to AKT-inhibition can be non-invasively assessed (31). We have also previously reported on HER3P1 imaging, showing that imaged Ga68 HER3P1 uptake correlates closely with HER3 expression as assessed by Western blot (23).

We extend on our prior findings by comparing Ga-68 HER3P1 imaging in two HER2 + breast cancer mouse models known to be resistant to HER2 inhibition with lapatinib (MDA-MB-453 and HCC-1569). While both HER2 + cell lines we selected for imaging are resistant to HER2 inhibition, only MDA-MB-453 demonstrates significant increase in HER3 expression. With Ga-68 HER3P1 imaging, we find that Ga-68 HER3P1 uptake increases in the MDA-MB-453 tumors nearly three fold after two days of treatment with lapatinib relative to pre-treatment imaging but remains the same in HCC-1569 tumors.

Of note, this observed increased in Ga-68 HER3P1 uptake in the MDA-MB-453 model in vivo was significantly greater than the increase in HER3 expression observed via Western blot in the same cell line. These data may speak to the multifactorial handling of HER3 cycling and processing – whereby increased trafficking and recycling of the HER3 receptor could contribute as much or more to increased

signaling through HER3 as increased expression(18). This difference in HER3 increase between our two studied cell lines in response to HER2 inhibition suggests different mechanisms of HER2 inhibitor resistance, and indeed HCC-1569 resistance to HER2 inhibition is rather mediated by PTEN loss(28), such that an increase in HER3 expression would not be expected. While the sum of our imaging data highly suggests that increased Ga68-HER3P1 uptake in MDA-MD-453 is reflective of increased HER3 expression and trafficking, we cannot entirely exclude the possibility that an increase in permeability also contributes to increased uptake, although were this the case would anticipate that HCC-1569 tumors would also demonstrate increased uptake post lapatinib.

We additionally hypothesized that tumor cell lines that upregulate HER3 expression in response to HER2 inhibition would be sensitive to additional HER3 inhibition, whereas tumor cell lines that do not increase HER3 expression under similar treatment conditions would not. In this context we suggest the potential therapeutic relevance of Ga68-HER3P1 PET imaging by showing that the HER3 upregulating MDA-MB-453 cell line is sensitive to the combination of HER3-downregulating siRNA and lapatinib, whereas HCC-1569 cells are insensitive. We suggest with these findings that HER3P1 PET imaging could be used to identify patients whose tumors utilize dynamic HER3 upregulation to resist HER2 inhibition and thereby those patients most likely to benefit by the addition of a HER3 inhibitor to their therapeutic regimen.

It is not known what percentage of HER2 + breast cancers upregulate HER3 in response to HER2 inhibition. A study of patients treated with two weeks of neo-adjuvant lapatinib prior to surgery found a wide-range of changes in HER3 mRNA post treatment compared to pre-treatment biopsy, from − 28% to + 78% across 17 patients with HER2 + breast cancers(32). This study found that HER3 mRNA increased non-significantly with response as measured by Ki-67 staining of resected specimens. Recognizing that mRNA is not the only mechanism by which cell-surface HER3 expression is increased, this small study sample provides indirect evidence that changes in HER3 expression may be a resistance mechanism employed by a subset of tumors to resist HER2 inhibition. In an additional study matched pre- and post-treatment biopsies in 8 patients with HER2 + tumors treated with 2 weeks of lapatinib showed upregulation of HER3 post-treatment by 135% as assessed by IHC (20).

The strong preclinical evidence for the role of HER3 in mediating resistance to HER2 treatment led to the development of several HER3-specific antibodies that have been evaluated preclinically and entered clinical trials(33–35). These antibodies have been evaluated as either single agents, in combination with chemotherapy, or with HER2 or EGFR inhibitors in several different oncologic indications. Most of these studies have had disappointing clinical results, although a recent Phase I study of U3-1402, a HER3 antibody – topoisomerase inhibitor conjugate, has reported positive preliminary data(36).

That the clinical trial results appear so at odds with the preclinical evidence may speak to two critical points that argue for the value of a noninvasive method of assessing tumoral HER3 expression: A) Dynamic increase in HER3 expression likely mediates HER2 inhibitor resistance in only a subset of HER2 + breast cancer patients; B) It has been very challenging to identify this subset of patients in whom this resistance process is active – as the dynamic increase in HER3 is seen only by comparing pre-treatment

HER3 expression to on-treatment expression. To identify this process in action requires both pre-treatment and on-treatment biopsies, which can be challenging to acquire. HER3 PET imaging may significantly improve our ability to observe dynamic upregulation of HER3, acting as a noninvasive predictive biomarker in future trials.

The role of antibody-based HER3 imaging agents have already undergone initial exploration. In a small clinical study, a Zr89 labelled anti-HER3 mAB (GSK2849330) was used to assess biodistribution and target engagement of antibody (37). Imaging with antibody based agents coupled with long-lived radionuclides such as Zr89 or Cu64 limits the ability to assess changes in HER3 expression due to the agents long half-lives. By contrast, HER3 PET imaging with a short-lived radiopharmaceutical such as Ga68-HER3P1 allows for repeat non-invasive assessment of tumoral HER3 expression over a short time scale. We can assess total HER3 expression across all tumor sites prior to therapy and then identify changes in HER3 expression that occur with targeted inhibition of HER2 or other targeted inhibitors within days of therapy initiation. The ability to noninvasively assess changes in HER3 expression across all tumor sites could allow for routine assessment of changes in HER3 without subjecting patients to repeat invasive biopsy, helping to readily identify those patients in whom a HER3 inhibitor may be of real clinical benefit. Our in vitro data demonstrating the benefit of additional HER3 knockdown only in cell lines that upregulate HER3 in response to HER2 inhibition with lapatinib supports this point. Of note, as we have only evaluated the role of Ga-68 HER3P1 imaging with lapatinib, it remains unknown if it would have a similar role in evaluated dynamic in increase in HER3 expression mediated by other HER2 inhibitor therapies such as trastuzumab or pertuzumab, especially considering the possible role of pertuzumab interfering with HER family heterodimerization(38). Additionally, it is worth noting that we have only evaluated changes in HER3 that occur rapidly with HER2 inhibitor initiation. This study does not evaluate the role that HER3 PET imaging may have in understanding mechanisms of resistance that occur with long-term treatment, only intrinsic resistance mechanisms.

We believe that Ga68-HER3P1 PET imaging could enable a paradigm shift in how HER3 inhibitor therapies are evaluated. The efficacy of HER3 inhibitor addition to targeted therapy should be evaluated in the context of a pre- and on-treatment HER3 PET imaging. Our preclinical study provides evidence that patients demonstrating an increase in on-treatment HER3 expression are those in whom the HER3 up-regulating resistance mechanism is most active and identifies those patients most likely to benefit by HER3 inhibitor addition.

Conclusion

We show in preclinical HER2 + breast cancer models that HER3 PET imaging using a dual timepoint pre- and on-treatment imaging paradigm allows for assessment of the dynamic changes in HER3 expression that occur with HER2 inhibition from lapatinib. We further show that cancers that dynamically upregulate HER3 in response to lapatinib inhibition are sensitive to additional HER3 siRNA knockdown whereas tumors that show no change in HER3 expression are not. We conclude from these data that HER3 PET

imaging could be used to identify those HER2 + breast cancers that would benefit most from HER3 inhibitor addition.

Declarations

Ethics approval: All studies were approved by the Massachusetts General Hospital Institutional Animal Care and Use Committee.

Consent for Publication: Not applicable

Availability of data and materials: The datasets used and/or analysed during the current study are available from the corresponding author on reasonable request

Competing Interests: The authors declare no competing interests

Funding: Funding for conduct of the study is provided by the American Society of Clinical Oncology Conquer Cancer Foundation Young Investigator Award (EWK), the Radiological Society of North American Research and Education Foundation Fellow Research Grant (EWK), and RO1 CA211233 (UM). The funding bodies had no role in design, data collection or analysis, interpretation, or writing of the manuscript.

Authors Contributions: Experimental conception and design was performed by EWK, BL, UM. Western blot and cell viability experiments were performed and analyzed by EWK and TK. Mouse biodistribution and PET imaging experiments were performed and analyzed by EWK, SN, and EA. siRNA experiments were performed and analyzed by NS. Manuscript drafting performed by EWK. Manuscript editing performed by EWK, NS, BL, UM. All authors read and approved the final manuscript

References

1. Slamon DJ, Leyland-Jones B, Shak S, Fuchs H, Paton V, Bajamonde A, et al. Use of chemotherapy plus a monoclonal antibody against HER2 for metastatic breast cancer that overexpresses HER2. N Engl J Med. 2001;344(11):783–92.
2. Swain SM, Baselga J, Kim SB, Ro J, Semiglazov V, Campone M, et al. Pertuzumab, trastuzumab, and docetaxel in HER2-positive metastatic breast cancer. N Engl J Med. 2015;372(8):724–34.
3. Verma S, Miles D, Gianni L, Krop IE, Welslau M, Baselga J, et al. Trastuzumab emtansine for HER2-positive advanced breast cancer. N Engl J Med. 2012;367(19):1783–91.
4. Geyer CE, Forster J, Lindquist D, Chan S, Romieu CG, Pienkowski T, et al. Lapatinib plus capecitabine for HER2-positive advanced breast cancer. N Engl J Med. 2006;355(26):2733–43.
5. Martin M, Holmes FA, Ejlertsen B, Delaloge S, Moy B, Iwata H, et al. Neratinib after trastuzumab-based adjuvant therapy in HER2-positive breast cancer (ExteNET): 5-year analysis of a randomised, double-blind, placebo-controlled, phase 3 trial. Lancet Oncol. 2017;18(12):1688–700.

6. Balduzzi S, Mantarro S, Guarneri V, Tagliabue L, Pistotti V, Moja L, et al. Trastuzumab-containing regimens for metastatic breast cancer. Cochrane Database Syst Rev. 2014;6:CD006242.
7. Swain SM, Clark E, Baselga J. Treatment of HER2-positive metastatic breast cancer. N Engl J Med. 2015;372(20):1964–5.
8. Smyth LM, Piha-Paul SA, Won HH, Schram AM, Saura C, Loi S, et al. Efficacy and Determinants of Response to HER Kinase Inhibition in HER2-Mutant Metastatic Breast Cancer. Cancer Discov. 2019.
9. Berns K, Horlings HM, Hennessy BT, Madiredjo M, Hijmans EM, Beelen K, et al. A functional genetic approach identifies the PI3K pathway as a major determinant of trastuzumab resistance in breast cancer. Cancer Cell. 2007;12(4):395–402.
10. Chandarlapaty S, Sakr RA, Giri D, Patil S, Heguy A, Morrow M, et al. Frequent mutational activation of the PI3K-AKT pathway in trastuzumab-resistant breast cancer. Clin Cancer Res. 2012;18(24):6784–91.
11. Giuliano M, Hu H, Wang YC, Fu X, Nardone A, Herrera S, et al. Upregulation of ER Signaling as an Adaptive Mechanism of Cell Survival in HER2-Positive Breast Tumors Treated with Anti-HER2 Therapy. Clin Cancer Res. 2015;21(17):3995–4003.
12. Hanker AB, Garrett JT, Estrada MV, Moore PD, Ericsson PG, Koch JP, et al. HER2-Overexpressing Breast Cancers Amplify FGFR Signaling upon Acquisition of Resistance to Dual Therapeutic Blockade of HER2. Clin Cancer Res. 2017;23(15):4323–34.
13. Liu L, Greger J, Shi H, Liu Y, Greshock J, Annan R, et al. Novel mechanism of lapatinib resistance in HER2-positive breast tumor cells: activation of AXL. Cancer Res. 2009;69(17):6871–8.
14. Scaltriti M, Eichhorn PJ, Cortes J, Prudkin L, Aura C, Jimenez J, et al. Cyclin E amplification/overexpression is a mechanism of trastuzumab resistance in HER2 + breast cancer patients. Proc Natl Acad Sci U S A. 2011;108(9):3761–6.
15. Soltoff SP, Carraway KL 3rd, Prigent SA, Gullick WG, Cantley LC. ErbB3 is involved in activation of phosphatidylinositol 3-kinase by epidermal growth factor. Mol Cell Biol. 1994;14(6):3550–8.
16. Amin DN, Sergina N, Ahuja D, McMahon M, Blair JA, Wang D, et al. Resiliency and vulnerability in the HER2-HER3 tumorigenic driver. Sci Transl Med. 2010;2(16):16ra7.
17. Sergina NV, Rausch M, Wang D, Blair J, Hann B, Shokat KM, et al. Escape from HER-family tyrosine kinase inhibitor therapy by the kinase-inactive HER3. Nature. 2007;445(7126):437–41.
18. Amin DN, Sergina N, Lim L, Goga A, Moasser MM. HER3 signalling is regulated through a multitude of redundant mechanisms in HER2-driven tumour cells. Biochem J. 2012;447(3):417–25.
19. Amin DN, Ahuja D, Yaswen P, Moasser MM. A TORC2-Akt Feed-Forward Topology Underlies HER3 Resiliency in HER2-Amplified Cancers. Mol Cancer Ther. 2015;14(12):2805–17.
20. Garrett JT, Olivares MG, Rinehart C, Granja-Ingram ND, Sanchez V, Chakrabarty A, et al. Transcriptional and posttranslational up-regulation of HER3 (ErbB3) compensates for inhibition of the HER2 tyrosine kinase. Proc Natl Acad Sci U S A. 2011;108(12):5021–6.

21. Arnould L, Gelly M, Penault-Llorca F, Benoit L, Bonnetain F, Migeon C, et al. Trastuzumab-based treatment of HER2-positive breast cancer: an antibody-dependent cellular cytotoxicity mechanism? Br J Cancer. 2006;94(2):259–67.
22. [Available from: https://clinicaltrials.gov/ct2/show/NCT03260491.
23. Larimer BM, Phelan N, Wehrenberg-Klee E, Mahmood U. Phage Display Selection, In Vitro Characterization, and Correlative PET Imaging of a Novel HER3 Peptide. Mol Imaging Biol. 2018;20(2):300–8.
24. Wetterskog D, Shiu KK, Chong I, Meijer T, Mackay A, Lambros M, et al. Identification of novel determinants of resistance to lapatinib in ERBB2-amplified cancers. Oncogene. 2014;33(8):966–76.
25. O'Brien NA, Browne BC, Chow L, Wang Y, Ginther C, Arboleda J, et al. Activated phosphoinositide 3-kinase/AKT signaling confers resistance to trastuzumab but not lapatinib. Mol Cancer Ther. 2010;9(6):1489–502.
26. Konecny GE, Pegram MD, Venkatesan N, Finn R, Yang G, Rahmeh M, et al. Activity of the dual kinase inhibitor lapatinib (GW572016) against HER-2-overexpressing and trastuzumab-treated breast cancer cells. Cancer Res. 2006;66(3):1630–9.
27. Koninki K, Barok M, Tanner M, Staff S, Pitkanen J, Hemmila P, et al. Multiple molecular mechanisms underlying trastuzumab and lapatinib resistance in JIMT-1 breast cancer cells. Cancer Lett. 2010;294(2):211–9.
28. Junttila TT, Akita RW, Parsons K, Fields C, Lewis Phillips GD, Friedman LS, et al. Ligand-independent HER2/HER3/PI3K complex is disrupted by trastuzumab and is effectively inhibited by the PI3K inhibitor GDC-0941. Cancer Cell. 2009;15(5):429–40.
29. Elkabets M, Vora S, Juric D, Morse N, Mino-Kenudson M, Muranen T, et al. mTORC1 inhibition is required for sensitivity to PI3K p110alpha inhibitors in PIK3CA-mutant breast cancer. Sci Transl Med. 2013;5(196):196ra99.
30. Garrett JT, Sutton CR, Kuba MG, Cook RS, Arteaga CL. Dual blockade of HER2 in HER2-overexpressing tumor cells does not completely eliminate HER3 function. Clin Cancer Res. 2013;19(3):610–9.
31. Wehrenberg-Klee E, Turker NS, Heidari P, Larimer B, Juric D, Baselga J, et al. Differential Receptor Tyrosine Kinase PET Imaging for Therapeutic Guidance. J Nucl Med. 2016;57(9):1413–9.
32. Coombes RC, Tat T, Miller ML, Reise JA, Mansi JL, Hadjiminas DJ, et al. An open-label study of lapatinib in women with HER-2-negative early breast cancer: the lapatinib pre-surgical study (LPS study). Ann Oncol. 2013;24(4):924–30.
33. Yonesaka K, Takegawa N, Watanabe S, Haratani K, Kawakami H, Sakai K, et al. An HER3-targeting antibody-drug conjugate incorporating a DNA topoisomerase I inhibitor U3-1402 conquers EGFR tyrosine kinase inhibitor-resistant NSCLC. Oncogene. 2019;38(9):1398–409.
34. Schoeberl B, Faber AC, Li D, Liang MC, Crosby K, Onsum M, et al. An ErbB3 antibody, MM-121, is active in cancers with ligand-dependent activation. Cancer Res. 2010;70(6):2485–94.

35. McDonagh CF, Huhalov A, Harms BD, Adams S, Paragas V, Oyama S, et al. Antitumor activity of a novel bispecific antibody that targets the ErbB2/ErbB3 oncogenic unit and inhibits heregulin-induced activation of ErbB3. Mol Cancer Ther. 2012;11(3):582–93.
36. Yonemori KMN, Takahashi S, Kogawa T, Nakayama T, Yamamoto Y, Takahashi M, Toyama T, Saeki T, Iwata H, editors Single Agent Activity Of U3-1402, a HER3-Targeting Antibody-Drug Conjugate, in HER3-Overexpressing Metastatic Breast Cancer: Updated Results From a Phase I/II Trial. Annals of Oncology 2019.
37. Menke-van der Houven. van Oordt CW, McGeoch A, Bergstrom M, McSherry I, Smith DA, Cleveland M, et al. Immuno-PET Imaging to Assess Target Engagement: Experience from (89)Zr-Anti-HER3 mAb (GSK2849330) in Patients with Solid Tumors. J Nucl Med. 2019;60(7):902–9.
38. Franklin MC, Carey KD, Vajdos FF, Leahy DJ, de Vos AM, Sliwkowski MX. Insights into ErbB signaling from the structure of the ErbB2-pertuzumab complex. Cancer Cell. 2004;5(4):317–28.

Figures

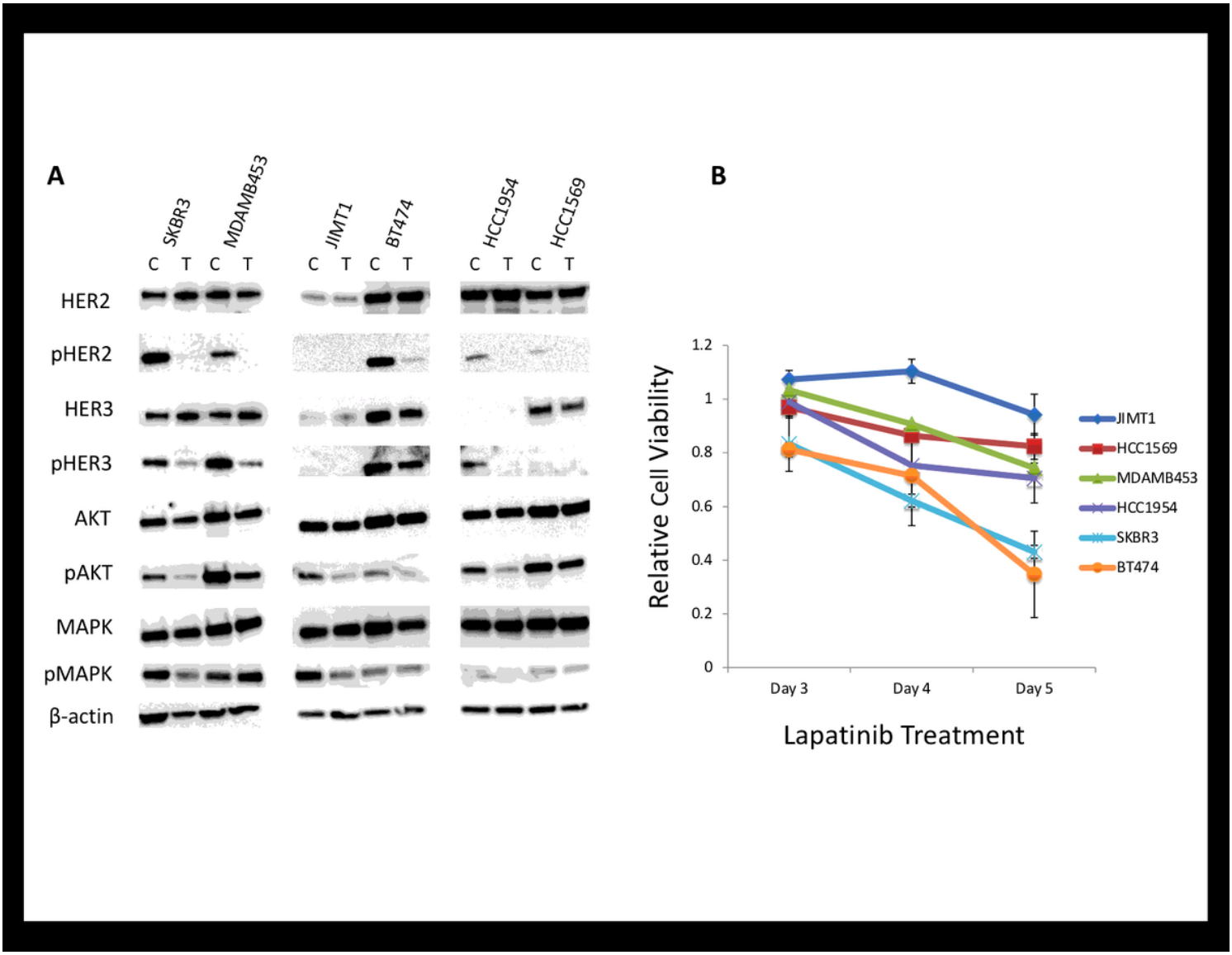

Figure 1

Changes in HER3 expression in panel of HER2+ breast cancer cell lines treated with lapatinib. Western blot of HER2+ breast cancer panel treated for 48h with the HER2 tyrosine kinase inhibitor lapatinib shows increase in HER3 expression with is not conserved across cell lines, consistent with HER3 upregulation being a mechanism of resistance in some but not all HER2+ tumors (A). HER2+ cells treated with 200 μM lapatinib for five days show that both sensitive cell lines (SKBR3, BT474) and resistant cell lines (MDMBA-453) demonstrate increase in HER3 expression (B).

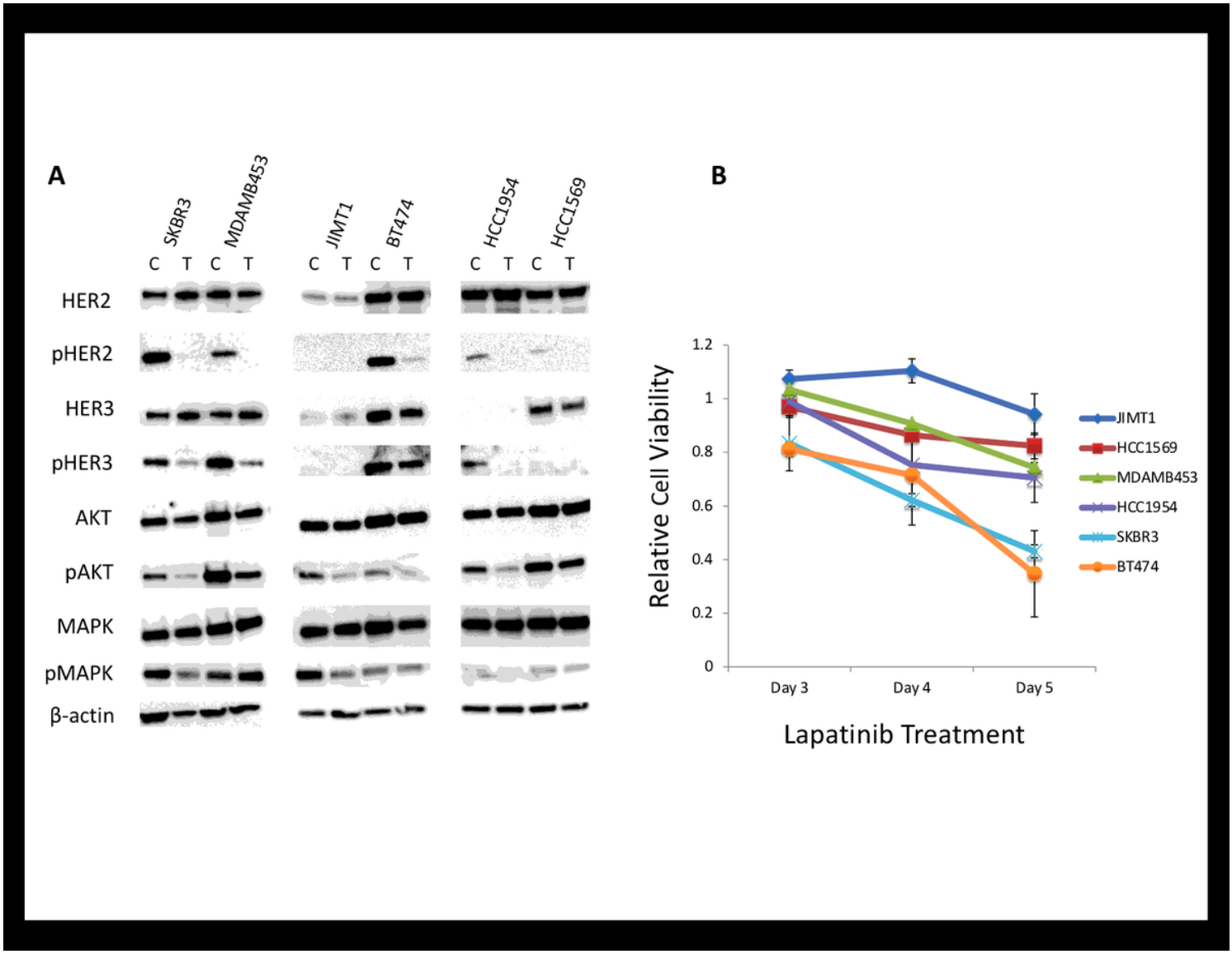

Figure 1

Changes in HER3 expression in panel of HER2+ breast cancer cell lines treated with lapatinib. Western blot of HER2+ breast cancer panel treated for 48h with the HER2 tyrosine kinase inhibitor lapatinib shows increase in HER3 expression with is not conserved across cell lines, consistent with HER3 upregulation being a mechanism of resistance in some but not all HER2+ tumors (A). HER2+ cells treated with 200 μM

lapatinib for five days show that both sensitive cell lines (SKBR3, BT474) and resistant cell lines (MD-MBA-453) demonstrate increase in HER3 expression (B).

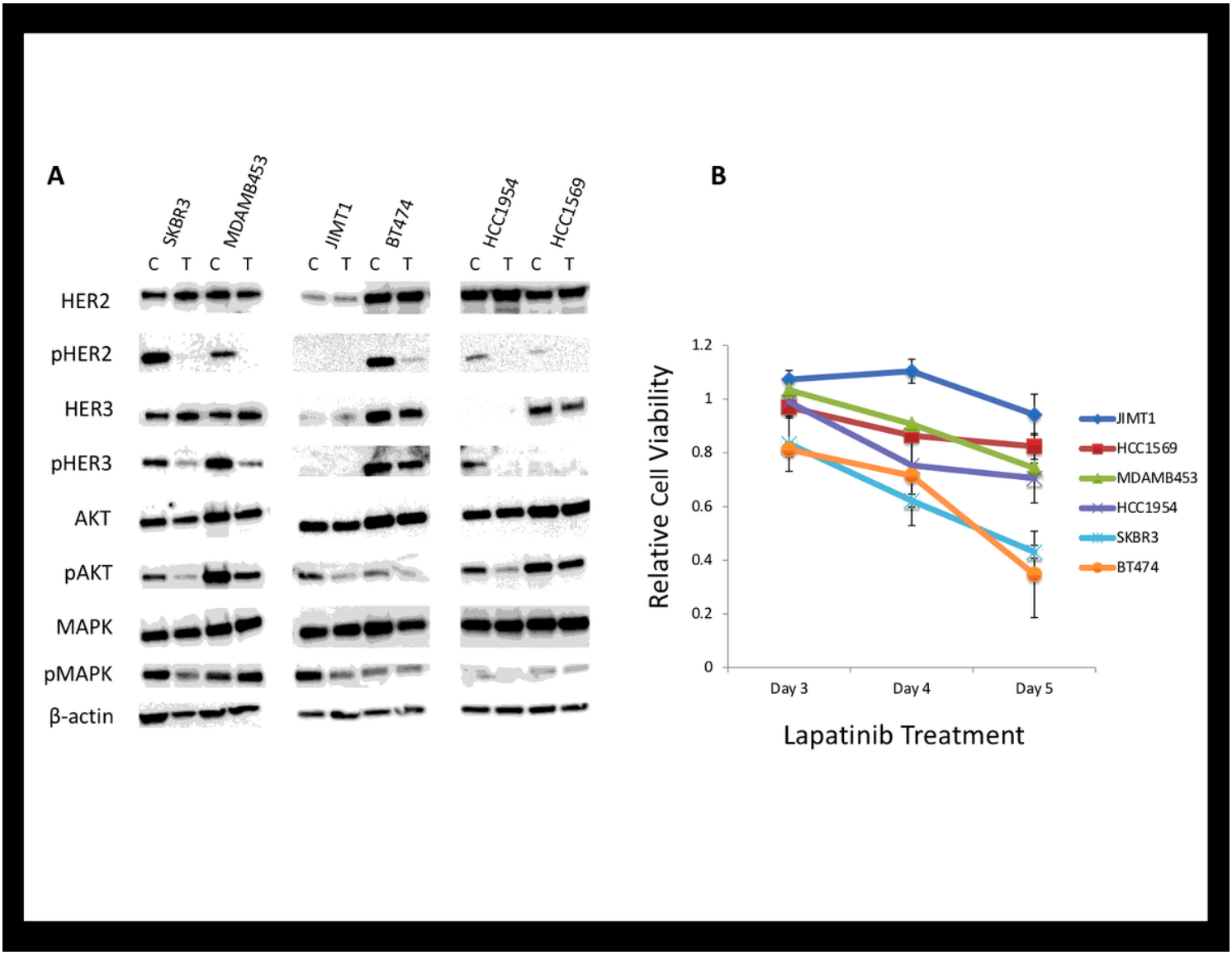

Figure 1

Changes in HER3 expression in panel of HER2+ breast cancer cell lines treated with lapatinib. Western blot of HER2+ breast cancer panel treated for 48h with the HER2 tyrosine kinase inhibitor lapatinib shows increase in HER3 expression with is not conserved across cell lines, consistent with HER3 upregulation being a mechanism of resistance in some but not all HER2+ tumors (A). HER2+ cells treated with 200 μM lapatinib for five days show that both sensitive cell lines (SKBR3, BT474) and resistant cell lines (MD-MBA-453) demonstrate increase in HER3 expression (B).

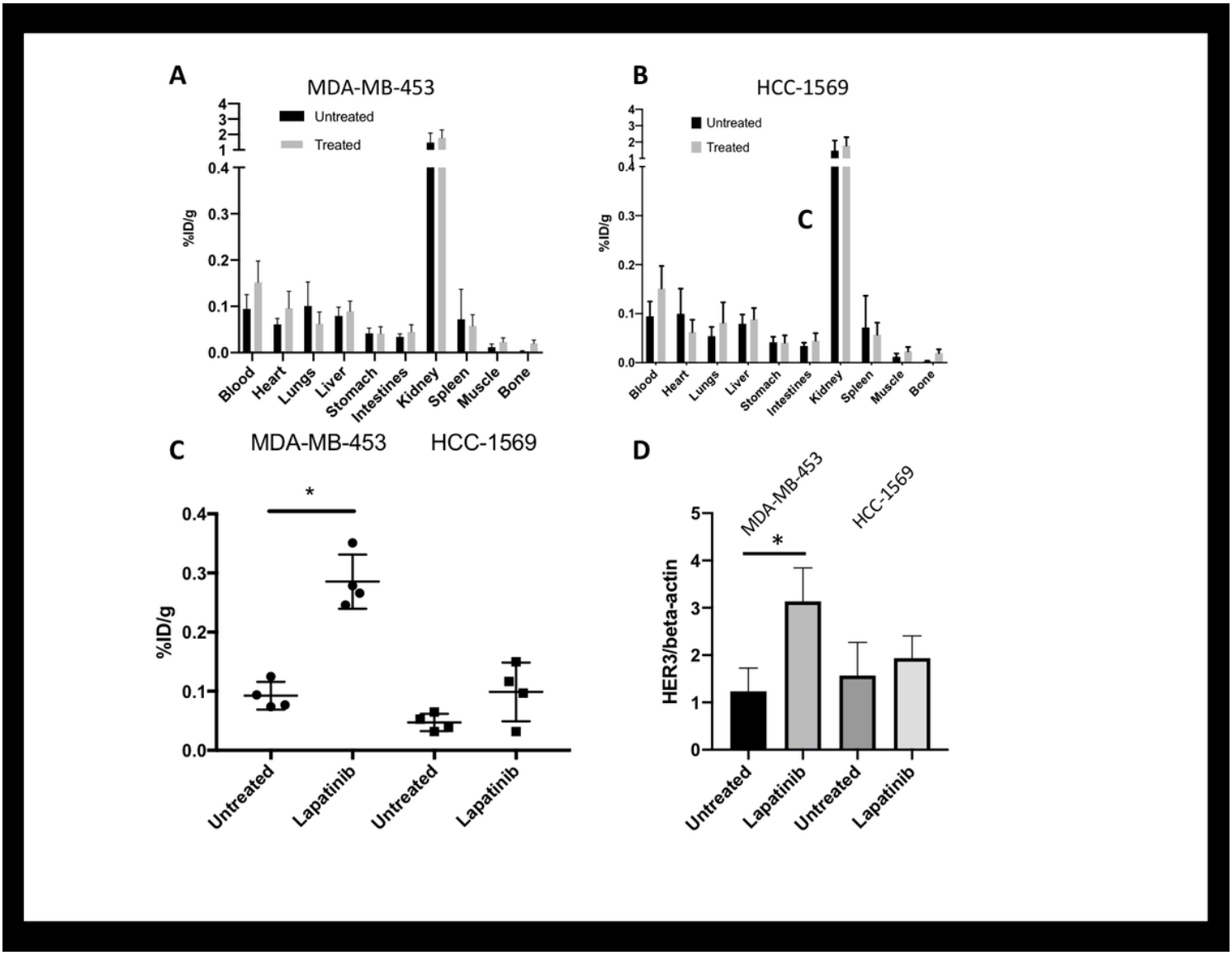

Figure 2

Ga68-HER3P1 Biodistribution in lapatinib treated and untreated mice implanted with MDA-MB-453 tumors and HCC-1569. Ga68-HER3P1 biodistribution at one hour post injection demonstrates primarily renal excretion with no significant differences between organ uptake pre and post treatment (A, B). Tumoral uptake is significantly increased in MDA-MB-453 tumors after treatment with lapatinib, with %ID/g increased approximately 3-fold (P=0.04) relative to vehicle treated mice. Change in HCC-1569 tumor uptake was non-significant (P=0.10) (C). Findings correlate with HER3 Western blot analysis of excised tumors, which shows a significant increase in HER3 in MDA-MB-453 tumors with treatment (P=0.04) but not in HCC-1569 treated tumors (P=0.45) (D).

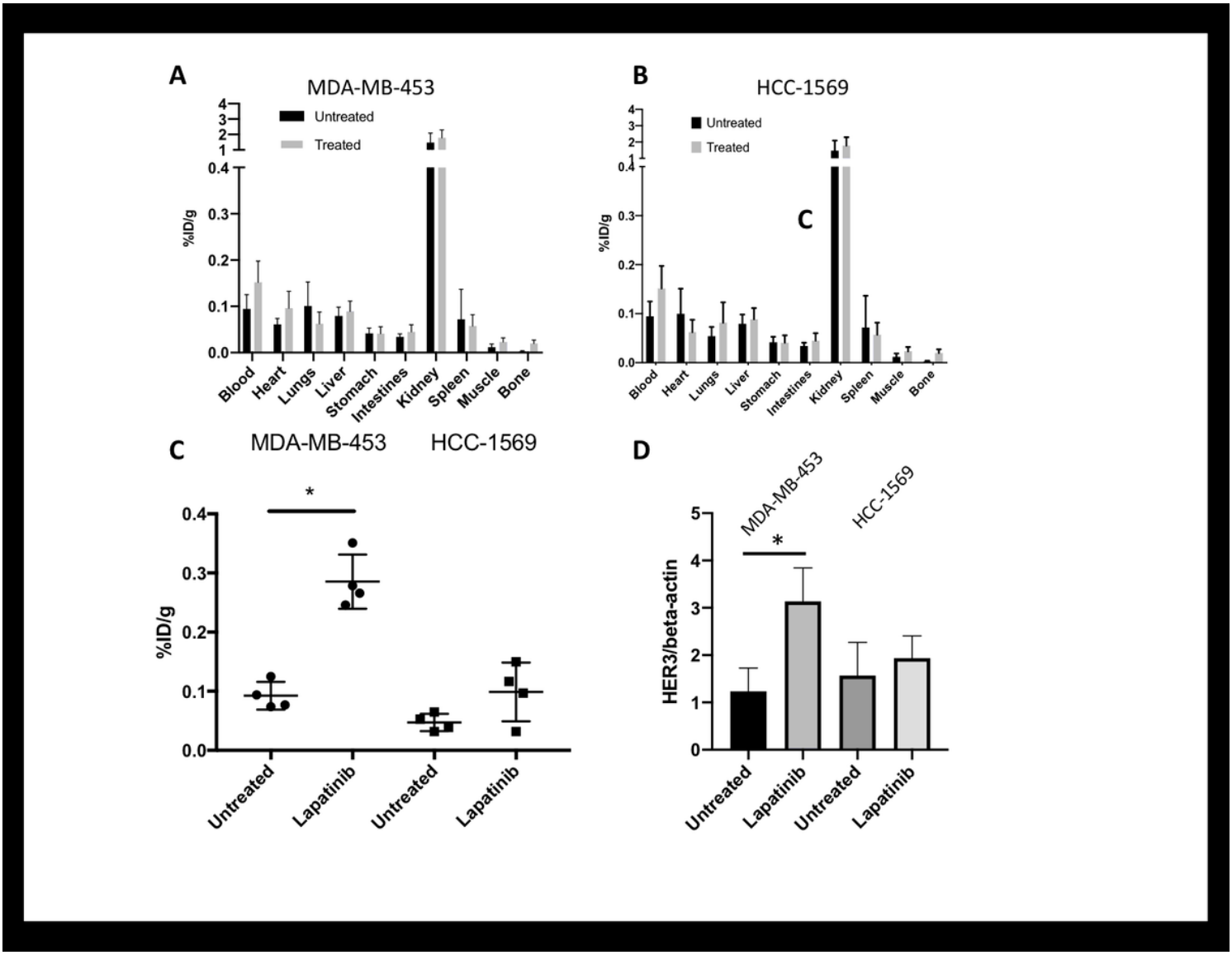

Figure 2

Ga68-HER3P1 Biodistribution in lapatinib treated and untreated mice implanted with MDA-MB-453 tumors and HCC-1569. Ga68-HER3P1 biodistribution at one hour post injection demonstrates primarily renal excretion with no significant differences between organ uptake pre and post treatment (A, B). Tumoral uptake is significantly increased in MDA-MB-453 tumors after treatment with lapatinib, with %ID/g increased approximately 3-fold (P=0.04) relative to vehicle treated mice. Change in HCC-1569 tumor uptake was non-significant (P=0.10) (C). Findings correlate with HER3 Western blot analysis of excised tumors, which shows a significant increase in HER3 in MDA-MB-453 tumors with treatment (P=0.04) but not in HCC-1569 treated tumors (P=0.45) (D).

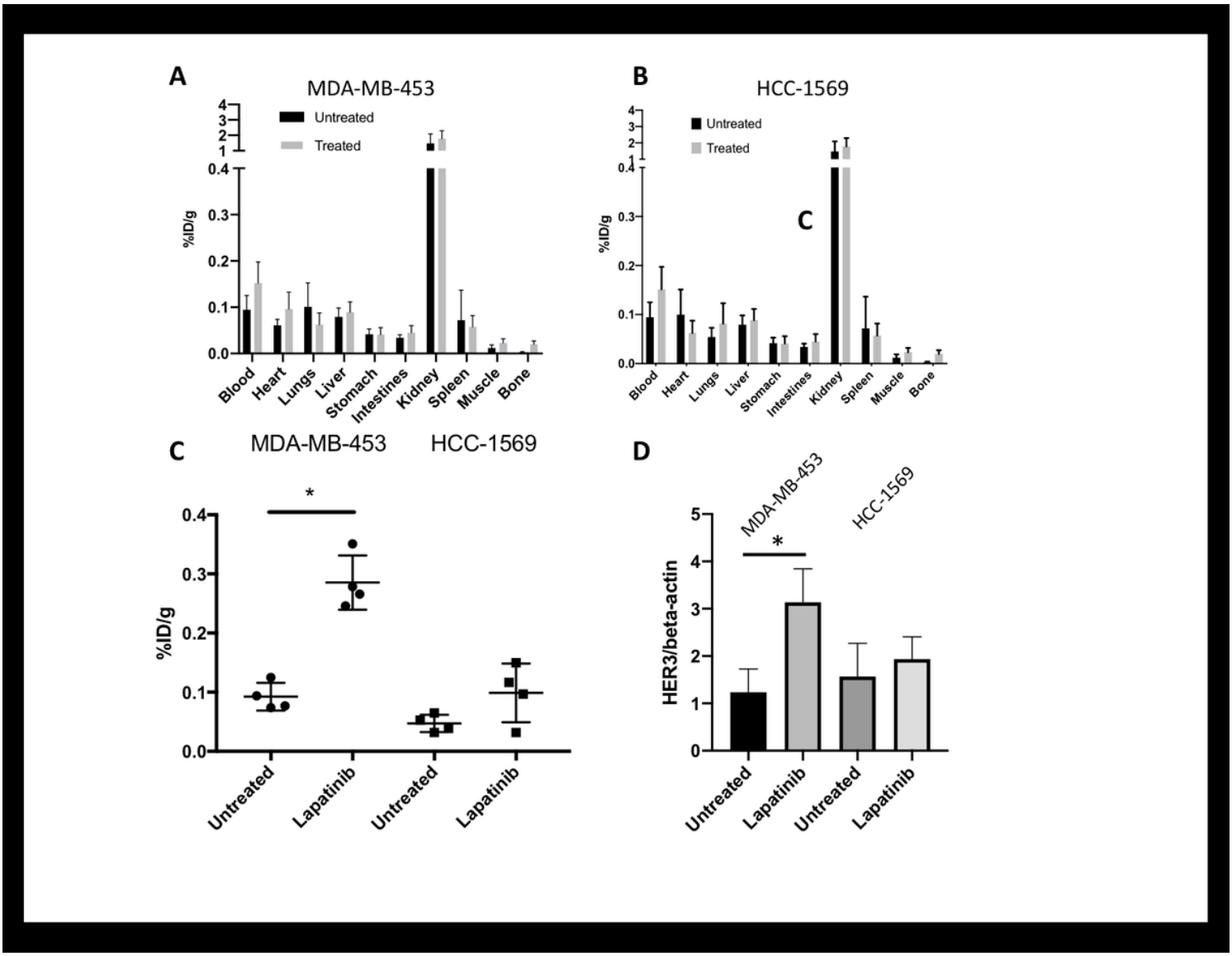

Figure 2

Ga68-HER3P1 Biodistribution in lapatinib treated and untreated mice implanted with MDA-MB-453 tumors and HCC-1569. Ga68-HER3P1 biodistribution at one hour post injection demonstrates primarily renal excretion with no significant differences between organ uptake pre and post treatment (A, B). Tumoral uptake is significantly increased in MDA-MB-453 tumors after treatment with lapatinib, with %ID/g increased approximately 3-fold (P=0.04) relative to vehicle treated mice. Change in HCC-1569 tumor uptake was non-significant (P=0.10) (C). Findings correlate with HER3 Western blot analysis of excised tumors, which shows a significant increase in HER3 in MDA-MB-453 tumors with treatment (P=0.04) but not in HCC-1569 treated tumors (P=0.45) (D).

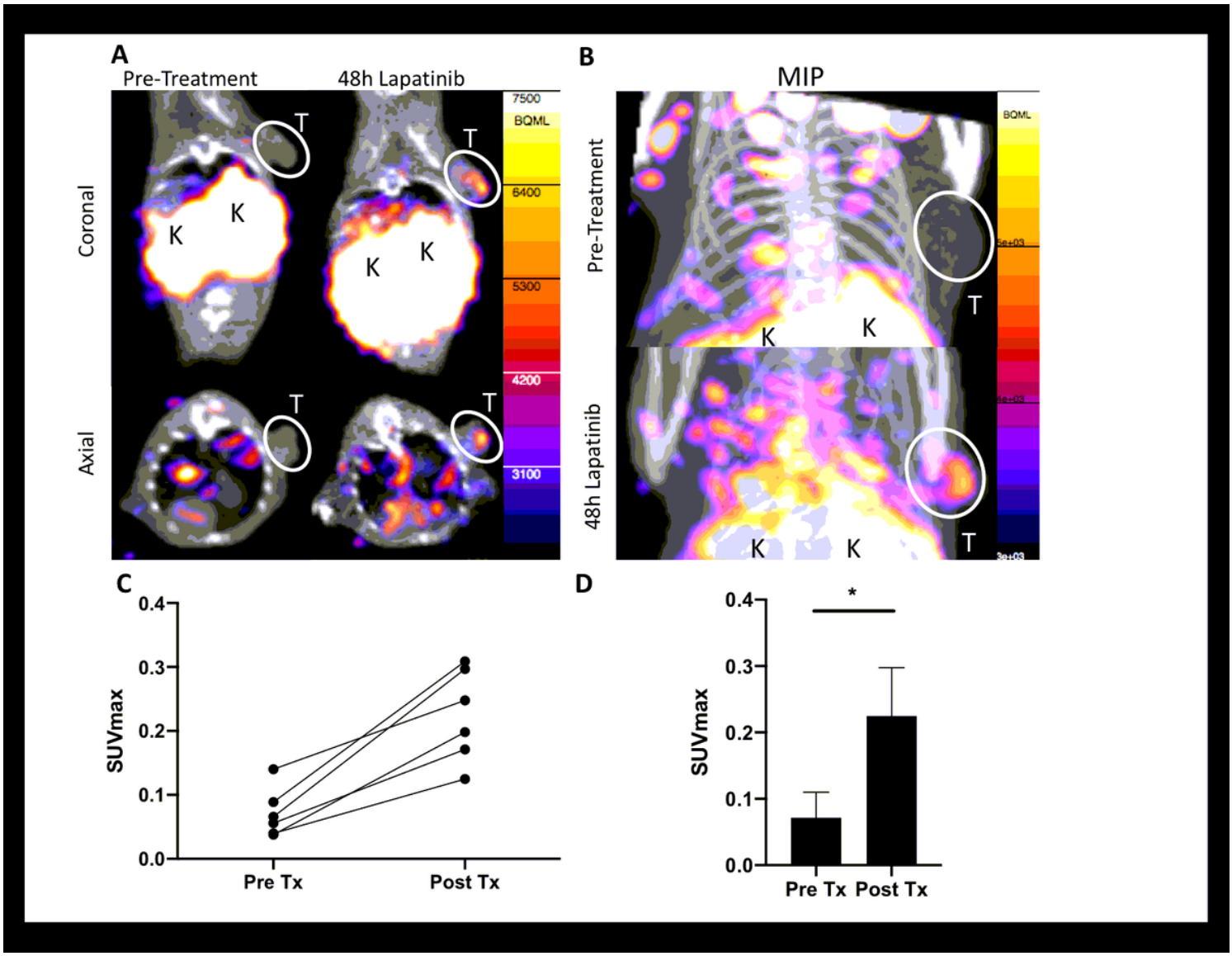

Figure 3

Ga68-HER3P1 repeat PET Imaging demonstrates HER3 uptake increase in individual mice with MDA-MB 453 tumors. The same mouse imaged pre and post 48h treatment with lapatinib demonstrates rapid increase in HER3 tracer uptake. Example coronal, axial, and MIP images (A) demonstrate readily discernable changes (tumor circled, T; kidneys, K). Line graphs demonstrate individual increase in imaged HER3 expression, as quantified by SUVmax in six imaged tumors (C). Group mean SUVmax increased from 0.07 pre-treatment to 0.24 post-treatment (P=0.002) (D). Note is made of lung uptake without CT-correlate that differs in configuration between pre and post treatment imaging that represents a combination of reconstruction artifact and 'bleed-through' from high renal uptake.

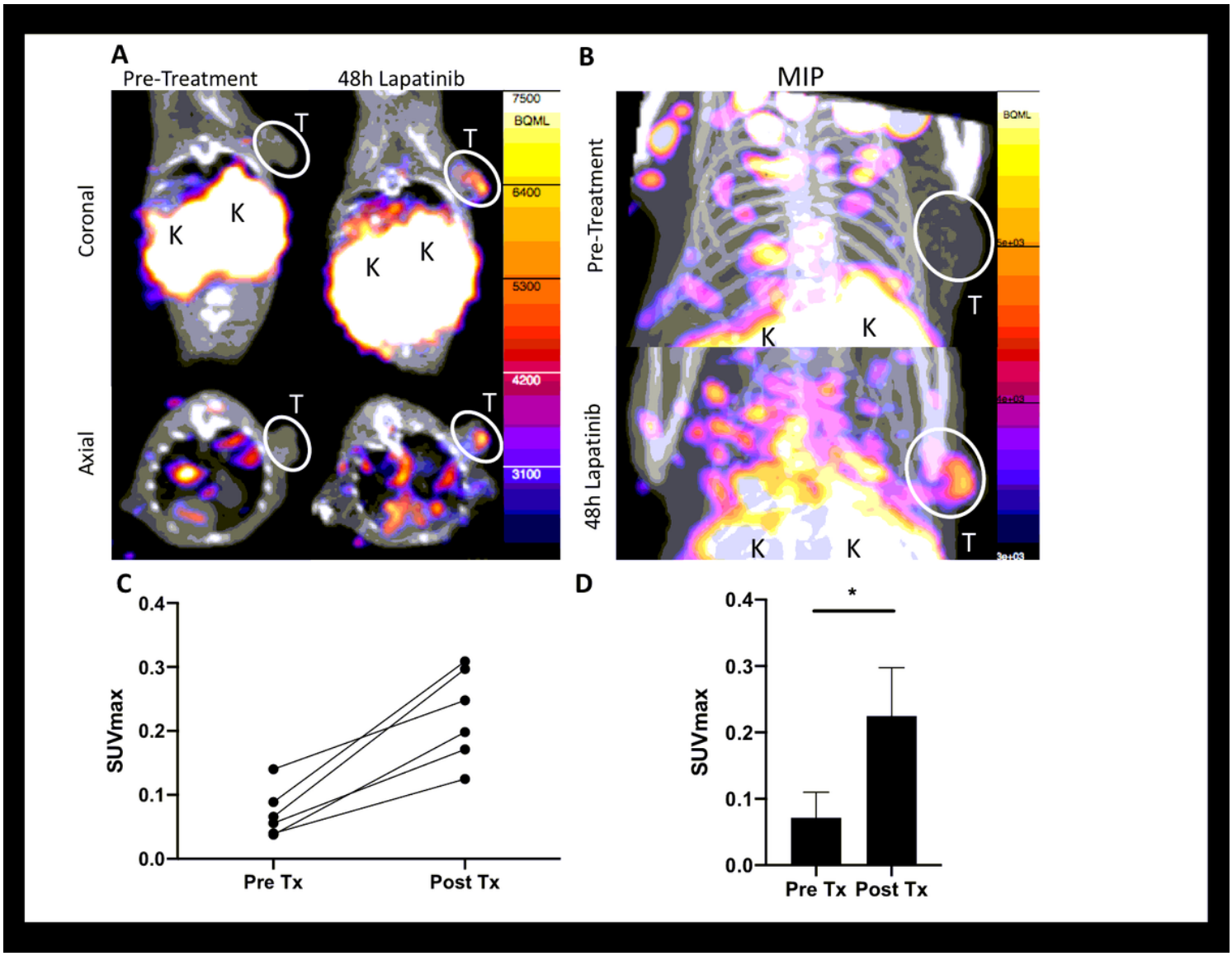

Figure 3

Ga68-HER3P1 repeat PET Imaging demonstrates HER3 uptake increase in individual mice with MDA-MB 453 tumors. The same mouse imaged pre and post 48h treatment with lapatinib demonstrates rapid increase in HER3 tracer uptake. Example coronal, axial, and MIP images (A) demonstrate readily discernable changes (tumor circled, T; kidneys, K). Line graphs demonstrate individual increase in imaged HER3 expression, as quantified by SUVmax in six imaged tumors (C). Group mean SUVmax increased from 0.07 pre-treatment to 0.24 post-treatment (P=0.002) (D). Note is made of lung uptake without CT-correlate that differs in configuration between pre and post treatment imaging that represents a combination of reconstruction artifact and 'bleed-through' from high renal uptake.

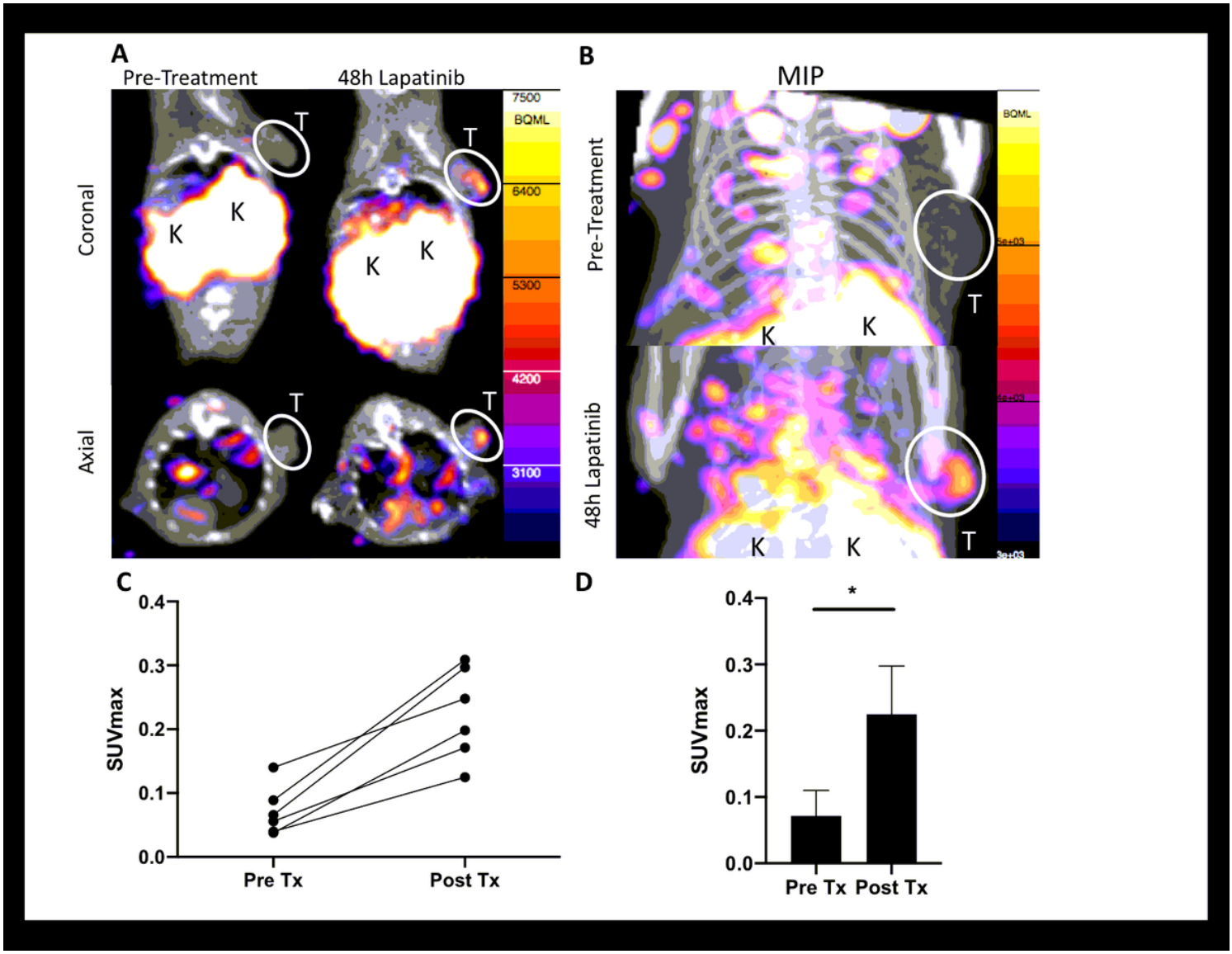

Figure 3

Ga68-HER3P1 repeat PET Imaging demonstrates HER3 uptake increase in individual mice with MDA-MB 453 tumors. The same mouse imaged pre and post 48h treatment with lapatinib demonstrates rapid increase in HER3 tracer uptake. Example coronal, axial, and MIP images (A) demonstrate readily discernable changes (tumor circled, T; kidneys, K). Line graphs demonstrate individual increase in imaged HER3 expression, as quantified by SUVmax in six imaged tumors (C). Group mean SUVmax increased from 0.07 pre-treatment to 0.24 post-treatment (P=0.002) (D). Note is made of lung uptake without CT-correlate that differs in configuration between pre and post treatment imaging that represents a combination of reconstruction artifact and 'bleed-through' from high renal uptake.

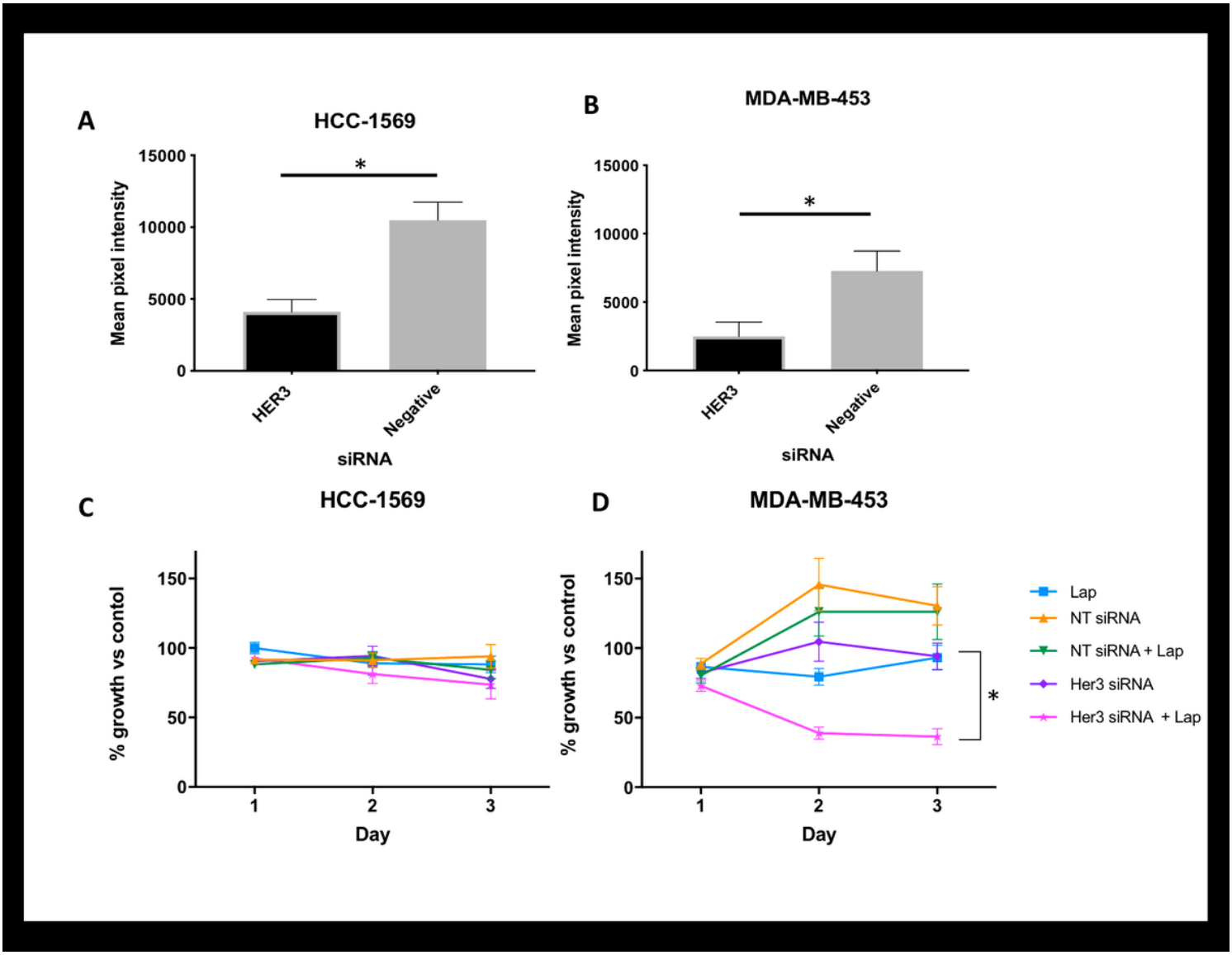

Figure 4

HER3 siRNA treatment improves response to lapatinib in MDA-MB-453 cells. Treatment with HER3 targeting siRNA significantly reduces HER3 mRNA relative to non-targeting siRNA (66% reduction for both cell lines, P=0.01) (A, B). HCC-1569 and MDA-MB-453 cells were treated with lapatinib, HER3 targeting siRNA, combination, or appropriate controls. HCC-1569 cell lines demonstrated no significant difference in response, regardless of treatment (P=0.6 for both comparisons) (C). MDA-MB-453 cell lines treated with lapatinib and HER3 siRNA demonstrated significantly less cell growth than mono-treated cell lines (37% for combination vs. 94% for both lapatinib-only and HER3 siRNA-only treated tumor) (P<0.001 for both comparisons) (D).

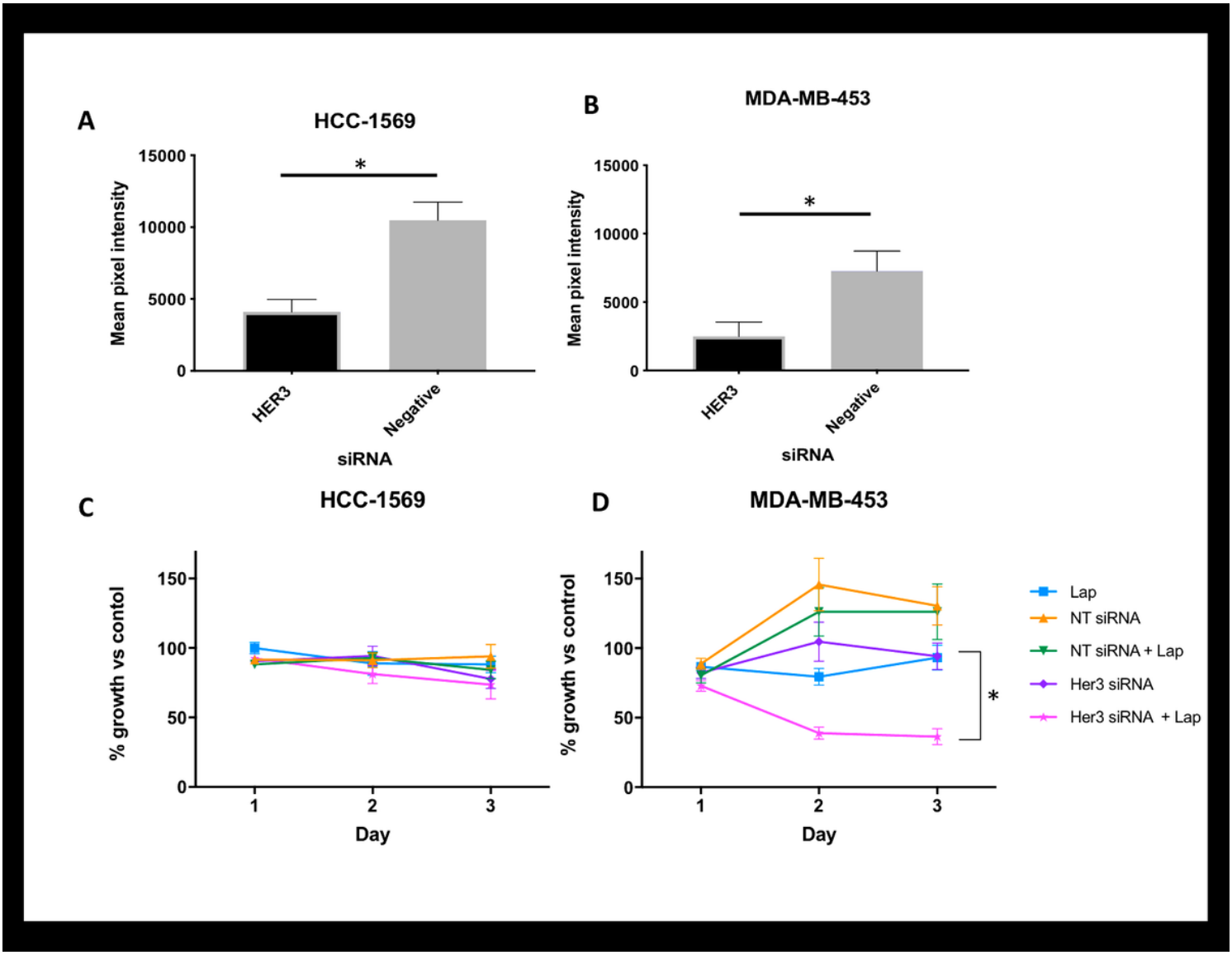

Figure 4

HER3 siRNA treatment improves response to lapatinib in MDA-MB-453 cells. Treatment with HER3 targeting siRNA significantly reduces HER3 mRNA relative to non-targeting siRNA (66% reduction for both cell lines, P=0.01) (A, B). HCC-1569 and MDA-MB-453 cells were treated with lapatinib, HER3 targeting siRNA, combination, or appropriate controls. HCC-1569 cell lines demonstrated no significant difference in response, regardless of treatment (P=0.6 for both comparisons) (C). MDA-MB-453 cell lines treated with lapatinib and HER3 siRNA demonstrated significantly less cell growth than mono-treated cell lines (37% for combination vs. 94% for both lapatinib-only and HER3 siRNA-only treated tumor) (P<0.001 for both comparisons) (D).

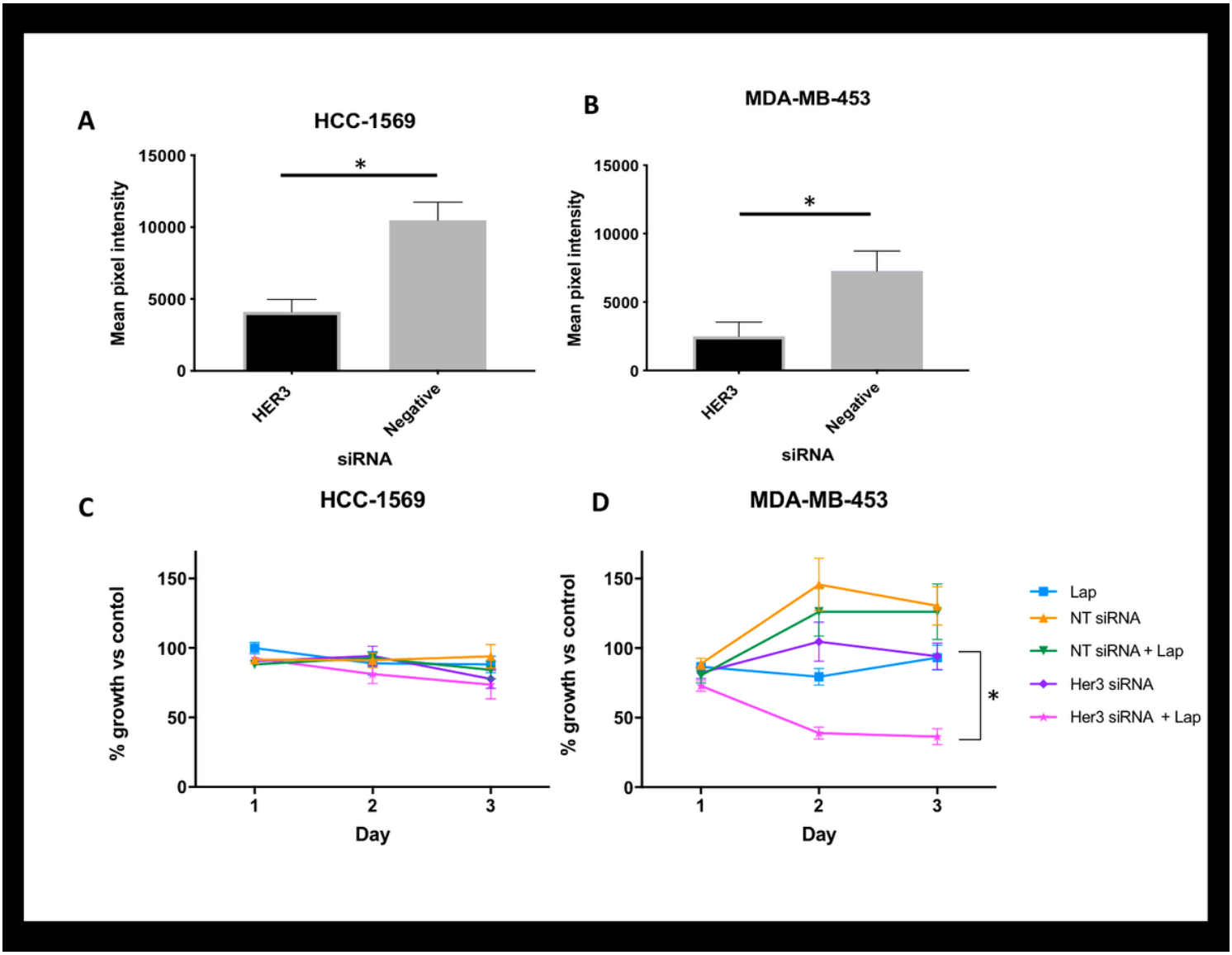

Figure 4

HER3 siRNA treatment improves response to lapatinib in MDA-MB-453 cells. Treatment with HER3 targeting siRNA significantly reduces HER3 mRNA relative to non-targeting siRNA (66% reduction for both cell lines, P=0.01) (A, B). HCC-1569 and MDA-MB-453 cells were treated with lapatinib, HER3 targeting siRNA, combination, or appropriate controls. HCC-1569 cell lines demonstrated no significant difference in response, regardless of treatment (P=0.6 for both comparisons) (C). MDA-MB-453 cell lines treated with lapatinib and HER3 siRNA demonstrated significantly less cell growth than mono-treated cell lines (37% for combination vs. 94% for both lapatinib-only and HER3 siRNA-only treated tumor) (P<0.001 for both comparisons) (D).